

RSC Advances



This is an *Accepted Manuscript*, which has been through the Royal Society of Chemistry peer review process and has been accepted for publication.

Accepted Manuscripts are published online shortly after acceptance, before technical editing, formatting and proof reading. Using this free service, authors can make their results available to the community, in citable form, before we publish the edited article. This *Accepted Manuscript* will be replaced by the edited, formatted and paginated article as soon as this is available.

You can find more information about *Accepted Manuscripts* in the [Information for Authors](#).

Please note that technical editing may introduce minor changes to the text and/or graphics, which may alter content. The journal's standard [Terms & Conditions](#) and the [Ethical guidelines](#) still apply. In no event shall the Royal Society of Chemistry be held responsible for any errors or omissions in this *Accepted Manuscript* or any consequences arising from the use of any information it contains.



An investigation on textural properties of mesostructured silica-based adsorbents for predicting CO₂ adsorption capacity

E. S. Sanz-Pérez,^a A. Arencibia,^a R. Sanz*^a and G. Calleja^a

Received 00th January 20xx,
Accepted 00th January 20xx

DOI: 10.1039/x0xx00000x

www.rsc.org/

Among the technologies proposed to reduce greenhouse gas emissions, adsorption with porous solids has been widely studied in the past years. Here, up to 30 inorganic porous adsorbents have been studied, obtaining their CO₂ uptake at 45 °C and ambient pressure, typical conditions of industrial post-combustion facilities after desulphurization step. A clear relationship between CO₂ adsorption capacity and the combination of surface area and sorbent affinity towards gas molecules through C parameter was found. This study provides novel findings that allow the prediction of CO₂ uptake in mesostructured silica physisorbents from their textural properties.

1. Introduction

Increasing CO₂ atmospheric concentrations have motivated intense research efforts in order to reduce greenhouse gas emissions. Carbon capture and storage (CCS) with solid sorbents has been abundantly proposed in the recent literature. A great variety of materials, such as mesostructured and amorphous silica, alumina, zeolites, metal-organic frameworks, polymers or carbonaceous sorbents have been considered.^{1,2,3,4,5} When non-functionalized materials like the ones cited above are used the adsorption mechanism is restricted to physisorption, although some selectivity towards CO₂ has been found in mixtures with N₂, O₂, H₂, CH₄ or Ar.^{6,7,8} This fact is explained by the CO₂ adsorption mechanism, which is caused by two different kinds of forces.⁹ On the one hand, non-specific van der Waals forces (namely dispersion and repulsion) are present whenever a molecule is adsorbed. On the other, there are specific adsorbent-adsorbate electrostatic interactions that take place only for certain compounds such as CO₂. This is due to its high quadrupole moment and its subsequent high polarizability.¹⁰ Physical adsorbents are generally characterized by their textural properties (mainly surface area, pore diameter and pore volume). For the assessment of surface area and related parameters, the model described by Brunauer-Emmett-Teller (BET)¹¹ is widely accepted.¹² Although there are several possibilities for the linearization of the original equation,¹³ the BET plot is commonly used following the original proposed linearization:

$$\frac{P}{n \cdot (P_0 - P)} = \frac{1}{n_m \cdot C} + P/P_0 \frac{C-1}{n_m \cdot C} \quad 1$$

where n is the amount of gas adsorbed at a given pressure (P); P_0 is the saturation pressure; n_m is the monolayer adsorption capacity; and C is a characteristic parameter.

Unlike Langmuir adsorption isotherm, the BET model assumes that adsorption is not ideal and multilayer formation can occur for low coverage.¹¹ This is also why adsorption in micropores is not accurately described by the BET equation, as multilayer adsorption in these narrow cavities is not possible.¹⁴ The BET model is still widely used due to its two main advantages: it is straightforward to apply and provides two of the most relevant textural magnitudes, i.e., the monolayer capacity, and the C parameter. The monolayer capacity refers to the moles of gas adsorbed in a monomolecular layer that covers the whole surface of the adsorbent, which allows the estimation of specific surface area, a parameter commonly used to compare adsorbents. In addition, the C parameter is a thermodynamical magnitude related to the enthalpy of adsorption, which is defined as:

$$C = \frac{a_1 v_2}{v_1 a_2} e^{(E_1 - E_L)/RT} \quad 2$$

where a is the condensation coefficient, i.e., the portion of incident adsorptive molecules that actually condense on the surface, v is the frequency of oscillation of the molecule in a direction normal to the surface, and E is the heat of adsorption. Subscript numbers indicate the adsorbed layer: 1 is the first adsorbed layer and 2 is the second one. As only two layers are considered, E_L is used rather than E_2 , referring to the liquefaction heat.¹¹ At the beginning, C was used to obtain approximate values for $(E_1 - E_L)$, i.e. the net heat of adsorption,

^a Department of Chemical and Energy Technology, ESCET. Universidad Rey Juan Carlos, C/ Tulipán s/n, 28933 Móstoles, Madrid, Spain.

* Raúl Sanz, corresponding author: raul.sanz@urjc.es

Electronic Supplementary Information (ESI) available: [Detailed experimental methodology, N₂ adsorption-desorption isotherms at 77 K and CO₂ adsorption-desorption isotherms at 45 °C]. See DOI: 10.1039/x0xx00000x

knowing that the ratio a_1v_2/v_1a_2 does not differ very much from the unity.¹⁵ However, the assumption that the heat of adsorption in the first layer (E_1) is independent of the amount of gas already adsorbed was early taken as untenable for the most active part of the surface.¹¹ Thus, the value obtained from E_1-E_L somewhat represents an average net heat of adsorption for the less active part of the adsorbing surface. Consequently, C parameter is currently used as an estimate of the adsorbent-adsorbate interaction energy rather than a quantitative measurement of the enthalpy of adsorption.¹⁶

Since physical adsorption is a surface-dependent process, the amount of gas adsorbed depends both on the available surface and on the adsorption potential.¹⁷ Thus, surface area and C parameter obtained by means of nitrogen adsorption have been widely used to explain catalytic and adsorption behaviour of materials. Actually, textural properties determined by N_2 adsorption are commonly correlated with the gas uptake of other adsorbates like Ar, H_2 , CH_4 or CO_2 . Surface area,^{18,19,20,21} pore and micropore volume,^{22,23,24} free volume,²⁵ pore shape, tortuosity and pore-structure irregularities,²⁶ or combinations of several N_2 -obtained properties^{27,28} have been successfully associated to the mass uptake of gasses other than N_2 .

Regarding CO_2 adsorption, some authors have reported correlations of the CO_2 uptake by mesostructured materials with their textural properties, finding higher CO_2 adsorption capacity for sorbents with larger surface area.^{29,30} A linear relationship between these variables was found for hybrid monolith aerogels of chitosan with increasing amounts of graphene oxide in their structure.³⁰

In this work, more than 30 different samples of adsorbents prepared from mesostructured solids have been studied in order to find a valid correlation between CO_2 adsorption capacity and textural properties such as available surface area, pore diameter, pore volume and adsorbate-adsorbent interactions (C parameter). Industrial post-combustion CO_2 capture equipment is usually located after the desulphurization unit. After this step, flue gas is released at 45–55 °C and 1 bar.³¹ Since this study has a very practical interest for carbon capture and storage purposes, 45 °C and 1 bar have been the conditions considered for CO_2 adsorption.

2. Experimental

2.1. Synthesis of siliceous materials

Materials of the families of conventional SBA-15,³² Al-SBA-15,³³ pore-expanded SBA-15 (SBA-PE),³⁴ conventional³⁵ and pore-expanded³⁶ MCM-41 and HMS³⁷ were considered. Several synthesis temperatures and surfactant removal techniques were used in order to obtain the different supports. All the adsorbents used in this work were synthesized following the procedures described in the Supporting Information, except Silica Gel (SG), purchased from Merk (Silica Gel 60 F₂₅₄).

2.2. Synthesis of amine-modified materials

Some functionalized adsorbents were also used in this study. SBA-15 synthesis route was modified to load aminopropyl-

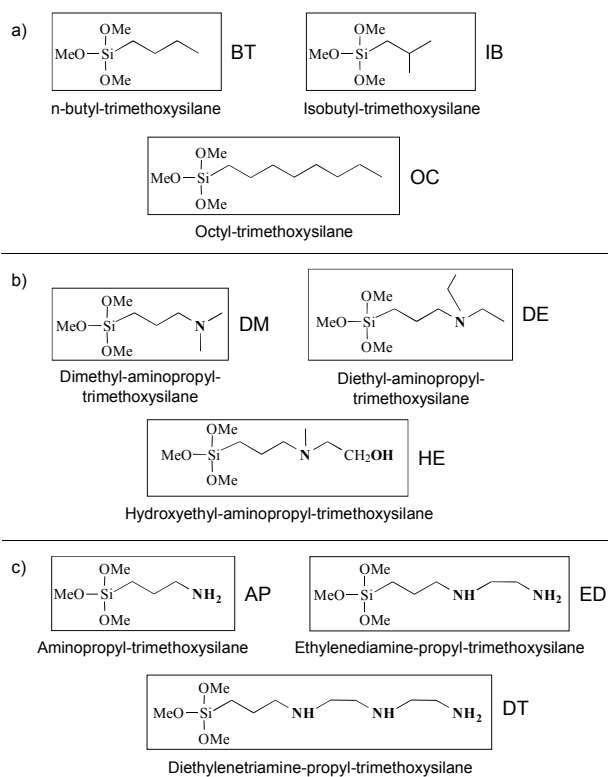


Fig 1 Molecular structures of organosilane precursors containing a) no amino groups, b) tertiary amino groups and c) primary and secondary amino groups.

trimethoxysilane (AP), ethylenediamine-trimethoxysilane (ED), and diethylenetriamine-trimethoxysilane (DT) organosilanes by co-condensation method. These organic molecules with one, two and three amino groups respectively yielded adsorbents named SBA-C-AP, SBA-C-ED and SBA-C-DT, where C indicates that the co-condensation method was followed. The structures of these organosilanes are shown in Figure 1.

Calcined SBA-15 was functionalized by grafting with the following silanes: butyl-trimethoxysilane (BT), isobutyl-trimethoxysilane (IB) and octyl-trimethoxysilane (OC), without amino groups in their structures; and (N,N-dimethylaminopropyl)-trimethoxysilane (DM), (N,N-diethylaminopropyl)-trimethoxysilane (DE) and N-hydroxyethyl-N-methylaminopropyl-trimethoxysilane (HE), with tertiary amino groups (see Figure 1 for structure details). Grafted materials were named SBA-*Org*, where *Org* refers to the type of organosilane used.

Detailed syntheses procedures and characterization techniques used can be found in the Supporting Information.

2.3. Physico-chemical characterization of supports

Prepared materials were characterized by low angle X-ray diffraction, using the $CuK\alpha$ monochromatic radiation in a powder diffractometer PHILIPS X-PERT MPD. Also, nitrogen adsorption-desorption isotherms at 77 K were obtained in a Micromeritics Tristar-3000 sorptometer. Siliceous materials were outgassed in N_2 flow for 8 h at a temperature of 200 °C, while the temperature was only of 150 °C for functionalized

samples in order to preserve their organic moieties. Elemental analyses of carbon, nitrogen and hydrogen were performed in a Vario EL III Elementar Analyzer System GMHB. CO₂ adsorption-desorption isotherms were obtained at 45 °C at pressures ranging from 0 to 6 bar by means of a VTI Scientific Instruments HVPA-100 volumetric equipment. All samples were outgassed at 110 °C for 2 h at a vacuum pressure of 5·10⁻³ mbar before and after each analysis. Two combined equilibration criteria were used to obtain isotherm points: a pressure drop below 0.2 mbar for 3 min or a maximum equilibration time of 50 min.

3. Results and discussion

3.1. Physical-chemical characterization

A complete characterization of the synthesized solids is presented in Table 1, including d_{100} and a_0 cell parameters measured by XRD, textural properties obtained by N₂ adsorption-desorption at 77 K as well as nitrogen content and total organic content measured by elemental analysis. Besides, a series of representative nitrogen adsorption-desorption isotherms is presented in Figure 2, the rest of them being shown in the Supporting Information (Figures SI 1 to SI 3). There is a wide diversity among the supports in terms of textural properties. Pore diameters are between 1.5 and 15.2 nm, in the range of mesopores or large micropores. Pore expanded SBA-PE-17e showed the highest pore diameter, up to 15.2 nm. Silica Gel (SG) has also large pores (10.2 nm) but

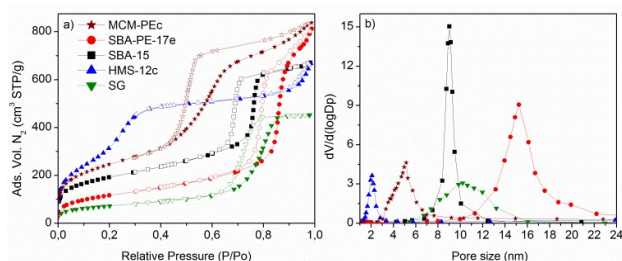


Fig 2 Textural characterization of SBA-15, SBA-PE-17e, HMS-12, MCM-PEc, and SG supports: a) N₂ adsorption-desorption isotherms at 77 K and b) BJH pore size distributions.

with a less defined pore size distribution. Conventional SBA-15 and pore-expanded MCM-41 exhibited well-defined pore sizes centered in 9.0 and 5.1 nm respectively. Finally, HMS-12c presents a so-called wormhole structure, with homogeneously sized pores but lacking any bi or tridimensional structure. C parameter values for calcined and ethanol-extracted SBA-15 are of 145 and 74 respectively (see Table 1). As detailed in the introduction section, C is related to the heat of adsorption (see Eq. 2). Hydrophilic materials present a high silanol (Si-OH) surface concentration and thus a strong interaction with N₂, resulting in high C values. The amount of silanol groups in silica has shown to be higher for extracted materials compared to calcined ones.^{38,39} Accordingly, a higher C value could be expected for extracted SBA-15e compared to calcined SBA-15. However, most of silanol groups in SBA-15e are hindered by the surfactant remaining after extraction (the organic content

Table 1 Textural properties, organic content and CO₂ adsorption capacity of the siliceous adsorbents considered.

Adsorbent	S_{BET}^a (m ² /g)	D_p^b (nm)	V_p^c (cm ³ /g)	C^a	d_{100}^d (nm)	a_0^e (nm)	e^f (nm)	Org ^g (wt. %)	N ^g (wt. %)	q (mg CO ₂ /g ads) ^h
SBA-15	692	9.0	1.03	145	10.5	12.1	3.1	-	-	21.2
SBA-15e	599	9.2	1.06	74	10.4	12.0	2.8	8.7	-	12.2
Al-SBA (60)	813	13.0	1.26	97	12.2	14.1	1.1	-	-	20.4
Al-SBA (30)	803	12.6	1.39	87	11.9	13.7	1.1	-	-	20.4
Al-SBA (10)	727	11.2	1.13	97	-	-	-	-	-	22.3
SBA-PE-17c	452	11.7	1.02	101	12.0	13.9	2.2	-	-	15.7
SBA-PE-12c	437	11.4	0.80	92	12.7	14.7	3.3	-	-	11.5
SBA-PE-17e	428	15.2	1.18	76	14.1	16.3	1.1	6.6	-	11.7
SBA-PE-12e	399	12.1	0.75	68	13.3	15.3	3.2	6.5	-	11.6
HMS-18c	643	1.7	0.59	62	-	-	-	-	-	12.0
HMS-16c	623	2.8	0.58	96	-	-	-	-	-	13.0
HMS-12c	1181	2.1	0.96	38	-	-	-	-	-	13.7
HMS-12e	1045	2.6	1.10	64	-	-	-	4.5	0.1	16.2
HMS-10c	918	2.1	0.72	48	-	-	-	-	-	14.8
HMS-8c	1056	1.5	0.72	39	-	-	-	-	-	15.9
MCM-41	1088	2.6	0.83	61	3.8	4.4	1.9	-	-	16.1
MCM-41e	684	2.4	0.54	44	4.3	5.0	2.6	22.1	1.0	9.3
MCM-PEc	894	5.1	1.28	99	4.9	5.6	0.5	-	-	15.1
SG	263	10.2	0.70	119	-	-	-	-	-	10.4

^a Specific surface and C parameter obtained by applying the BET equation in the P/P₀ range from 0.05 to 0.2. ^b Pore diameter obtained from BJH pore size distribution. ^c Single pore volume measured at a relative pressure of 0.96. ^d Interplanar spacing obtained from the X-ray diffractogram. ^e Unit cell calculated from d_{100} values. ^f Wall thickness calculated by subtracting D_p from a_0 . ^g Total organic content (hydrogen, carbon and nitrogen) and nitrogen content measured by Elemental Analysis. ^h CO₂ adsorption capacity obtained at 45 °C and 1 bar in a volumetric analyzer.

of SBA-15e is of 8.7 %). For calcined SBA-15, which is pure silica, all silanol groups are available to N₂ molecules, resulting in stronger interactions with N₂ and hence, in higher C parameter than extracted SBA-15e. SBA-PE and MCM-41 materials also show C values after calcination and extraction which are in agreement with this remark (see Table 1).

When the structure of SBA-15 is modified by enlarging pores (SBA-PE) or including Al atoms in the structure, C values decreased from 145 to 70-100. Thus, it can be deduced that the modified structures present a lower affinity towards N₂ molecules. This change can be ascribed to a loss of silanol groups or to a surface restructuring. The latter involves an increased surface roughness and reorientation of silanol groups leading to a lower surface polarity.⁴⁰

Textural parameters of adsorbents prepared by co-condensation with AP, ED and DT, and by grafting with organosilanes containing just tertiary amino groups (DE, DM and HE) or no amino groups at all (IB, BT, OC) are summarised in Table 2. As seen, specific surface, pore diameter and pore volume are considerably lower than those of SBA-15 as a consequence of the pore-filling after organic functionalization. Samples functionalized with amine-containing organosilanes also present a certain amount of nitrogen loaded (1.3-4.0 %). This variation is consistent with the decrease observed in the textural properties.

C parameter took values between 28 and 101, much smaller than the one corresponding to siliceous SBA-15, which was 145. This difference is in agreement with the previous results obtained for extracted materials, where the presence of organic content led to a weaker affinity between N₂ and the organically-covered sorbent surface and thus to lower C values. Even more, in this case there is not only an increase of organic content, but also a decrease in the silanol surface concentration due to the grafting of organosilanes.

3.2. CO₂ adsorption

Pure CO₂ adsorption-desorption isotherms obtained at 45 °C for a selection of siliceous and functionalized materials are displayed in Figure 3a and 3b respectively. The complete set of isotherms for all the adsorbents is shown in the Supporting Information (Figures SI 4 to SI 7).

The isotherms of non-functionalized supports are characteristic of physical adsorption, as previously described.⁴¹ The CO₂ uptake determined at 1 bar does not seem to correlate with textural properties (Table 1). For example, samples as different as SBA-PE-17e and HMS-18c, with no common features in their textural properties, presented analogous CO₂ uptakes, around 12 mg CO₂/g ads. Likewise, samples as similar as SBA-15 and SBA-15e showed very different CO₂ adsorption capacities, 21.2 and 12.2 mg CO₂/g ads respectively.

The functionalization of SBA-15 led to interesting findings (Figure 3b and Table 2). The grafting with organosilanes containing tertiary amino groups (DE, DM and HE) or no amino groups at all (IB, BT and OC) as well as the co-condensation of molecules with primary and secondary groups (AP, ED and DT)

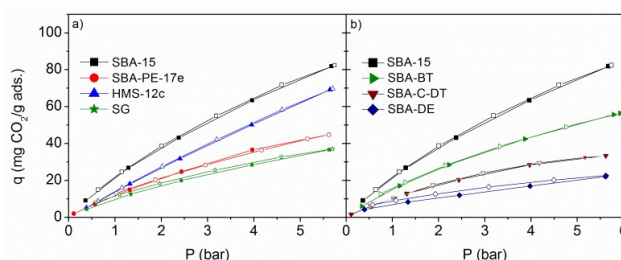


Fig 3 Pure CO₂ adsorption-desorption isotherms at 45 °C of a) bare supports SBA-15, SBA-PE-17e, HMS-12c and SG and b) functionalized SBA-15 adsorbents.

Table 2 Textural properties, organic content and CO₂ adsorption capacity (45 °C, 1 bar) of SBA-15 functionalized materials.

Adsorbent	S _{BET} (m ² /g)	D _p (nm)	V _p (cm ³ /g)	C	Org. (wt. %)	N (wt. %)	q (mg CO ₂ /g ads)
SBA-15	692	9.0	1.03	145	-	-	21.2
SBA-OC	621	8.2	0.92	88	5.3	-	17.0
SBA-BT	612	8.3	0.90	99	5.6	-	15.0
SBA-IB	650	8.5	0.97	101	4.1	-	16.8
SBA-DE	307	7.2	0.51	30	18.7	2.7	6.9
SBA-DM	266	7.4	0.47	28	16.2	3.1	4.6
SBA-HE	207	7.1	0.35	34	19.5	4.0	5.5
SBA-C-AP	572	8.2	0.87	68	4.7	1.3	10.1
SBA-C-ED	508	8.3	0.78	63	7.8	2.7	11.2
SBA-C-DT	477	8.1	0.41	57	7.3	2.6	10.2

resulted in adsorbents with a lesser CO₂ uptake than siliceous SBA-15. This result was originated by the surface reduction occurred during the functionalization process and the fact that no active groups for CO₂ adsorption were present in these samples. Silanes and functionalization methods were specifically selected in order to yield amine-modified adsorbents that only present physical adsorption of CO₂. Amines loaded by co-condensation (AP, ED and DT) using an acidic media are protonated⁴² and end up embedded in the silica walls, so they provide little interaction with CO₂.⁴¹ Besides, tertiary amines (DM, DE and HE) have been extensively described as not active for CO₂ adsorption in dry conditions.^{43,44} Figure 3b (and Figure SI 7) confirm that the shape of the CO₂ adsorption-desorption isotherms is clearly due to just physisorption. This is in agreement with many theoretical and experimental works that discard the occurrence of chemical adsorption on samples with analogous behaviour,^{45,46,47} thus ruling out the presence of chemical adsorption on the samples above described.

In order to present definite proof regarding the absence of chemical adsorption in the samples presented upon here, isosteric heat of adsorption was estimated for SBA-15 pure silica and SBA-C-ED. Experimental adsorption isotherms were acquired at 35, 45, 55 and 65 °C and modeled according to Sips equation (Eq. 3):⁴⁸

$$n = n_s \frac{(b \cdot P)^{1/n}}{1 + (b \cdot P)^{1/n}} \quad 3$$

where n and n_s are the number of moles adsorbed at a given

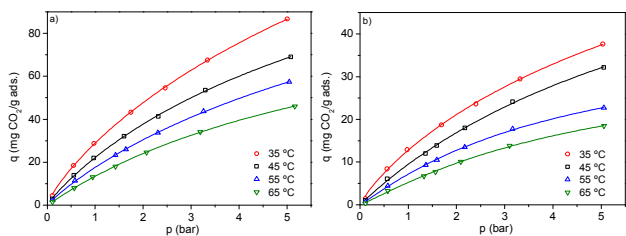


Fig 4 CO₂ adsorption equilibrium points at temperatures between 35 °C and 65 °C for a) SBA-15 silica and b) co-condensed SBA-C-ED with 2.7 %N. The lines correspond to the Sips isotherm model fit.

pressure P and the number of moles adsorbed at saturation, respectively, and b and t are constants. The constant t is generally considered as a heterogeneity factor.⁴⁹ Values higher than 1 are ascribed to heterogeneous systems, while values close to (or exactly) 1 indicate a material with relatively homogenous binding sites.⁵⁰

Figure 4 displays experimental adsorption points as well as the Sips isotherm model fits for SBA-15 and SBA-C-ED adsorbents. Suitable fittings with R^2 values around 0.999 were observed in all cases. Parameters included in Sips equation as well as R^2 fitting values for each isotherm are listed in Table S1 (Supporting Information).

Clausius-Clapeyron equation (Eq. 4) was used to obtain isosteric heat of adsorption, as shown in Figure SI 9.

$$Q_{st} = -R \left(\frac{\partial \ln P}{\partial (1/T)} \right)_i \quad 4$$

Finally, the isosteric heat of adsorption was plotted against CO₂ uptake, obtaining the curves presented in Figure 5. According to these results, isosteric heat of adsorption at the minimum coverage considered was of 33.6 and 36.5 kJ/mol for SBA-15 and SBA-C-ED respectively.

Values measured by calorimetry for mesoporous silicas have been reported to range between 20 and 35 kJ/mol,^{51,52,53} with these low values being associated to physical adsorption. On the contrary, samples with available amino groups from AP, ED and DT organosilanes showed much higher values, from 50 to 70 kJ/mol,^{53,54,55} being ascribed to chemical adsorption. Thus, it can be inferred that both SBA-15 silica and ED-containing SBA-C-ED are interacting with CO₂ just by physical adsorption. Contrasting with physical adsorbents presented in this work, many researchers use amines that actually react with CO₂, resulting in chemisorption processes. These materials achieve much higher CO₂ uptake^{53,56,57,58,59,60,61} and their CO₂ adsorption isotherms are very different to those described

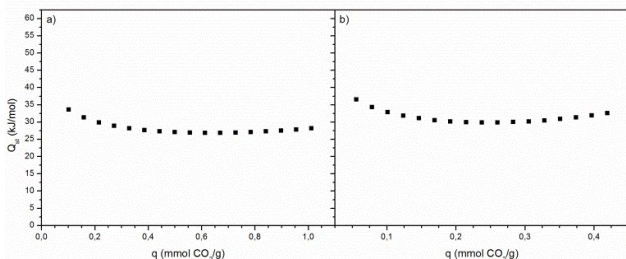


Fig 5 Isosteric heat of adsorption for CO₂ on a) siliceous SBA-15 and b) amine-containing SBA-C-ED.

here. Namely, the CO₂ uptake at low pressures is considerable, its dependence with pressure is much lower than in the case of physisorption and the reversibility of the process is not complete (i.e., adsorption and desorption branches do not overlap).^{41,45} When chemisorption strongly contributes to the overall CO₂ adsorption capacity, this variable is mainly governed by the kind, amount and distribution of amino groups loaded, as extensively reasoned in the literature.^{9,62,63,64,65} Since functionalized samples prepared in this work adsorb CO₂ only by physisorption, there is no dependence on any magnitude related to the amino groups loaded when such moieties are present.

3.3. Correlation between CO₂ uptake and textural properties

In an attempt to find a relationship between physical CO₂ adsorption and textural properties, the CO₂ uptake of all the adsorbents was plotted against the main magnitudes obtained from N₂ adsorption-desorption isotherms, i.e., specific surface area, pore diameter, pore volume and C parameter (Figure 6). As seen, these results reveal that none of these parameters individually considered correlates with the CO₂ uptake. Detailed fitting parameters are listed in Table 3, where very low values of the regression parameter R^2 are listed in the four first cases. This confirms that specific surface area, pore diameter, pore volume and C parameter are poor predictors of CO₂ uptake if considered individually.

In contrast with these results, many papers claim that pore diameter plays an important role in CO₂ adsorption.⁶⁶⁻⁶⁸ Though this statement is correct, it only applies to microporous adsorbents. On the contrary, mesoporous materials are formed by much wider pores and confinement effects are not significant. Consequently, there is no clear effect of this variable in the CO₂ uptake, as seen in Figure 6b.

For mesoporous adsorbents, Alhwaige et al. have recently

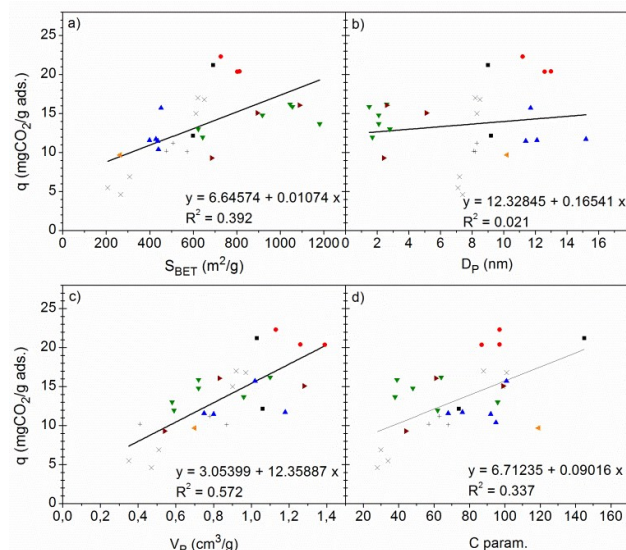


Fig 6 CO₂ uptake values (1 bar and 45 °C) as a function of a) BET specific surface, b) pore diameter, c) pore volume and d) C parameter. Linear regressions are plotted along with the numerical equation.

Legend: conventional SBA-15 (■), Al-SBA-15 (●), pore-expanded SBA-15 (▲), HMS (▼), Silica Gel (◄), MCM-41 (►), grafted SBA-15 (X) and co-condensed SBA-15 (+).

reported a robust linear correlation between CO₂ uptake and BET surface using a chitosan aerogel with different amounts of graphene oxide (GO), with GO being responsible of the increment detected in porosity.³⁰ However, the authors stated that chemisorption on GO active sites was likely the underlying adsorption mechanism, so there may be a chemisorption contribution to the overall CO₂ uptake in this case.

Regarding CO₂ physisorption, it is well known that the available surface area is very likely playing a role in CO₂ capture, although probably not as an individual variable. A similar conclusion was drawn by Xu and Hedin by using more than 30 microporous adsorbents.²⁹ These authors observed the influence of surface area in CO₂ adsorption but did not get a robust linear correlation, concluding that surface area was not predicting CO₂ uptake by itself.

Additionally, it is reasonable to assume that the surface chemistry is also a determining factor in the amount of gas adsorbed. In this study, C parameter is considered in order to quantify the affinity of a given surface towards an adsorptive. Despite C parameter is calculated from the N₂ adsorption isotherm it constitutes a fair approximation to the affinity between the adsorbent surface and the gas adsorbed by means of weak interactions. This assumption is coherent with the number of references correlating C parameter or BET surface area (both of them deriving from the BET equation) with the adsorption capacity of gases other than N₂.^{19,20,21} Thus, CO₂ uptake was fitted against the product of the available surface area (S_{BET}) and its affinity towards an adsorptive (C parameter). As shown in Figure 7, the points are

Table 3. Linear fittings between the CO₂ adsorption uptake at 45 °C and 1 bar and textural parameters.

x	Individual Fitting q(CO ₂) = a + k·x						
	R ²	Slope	Std. error	Perc. Error (%)	Intcp.	Std. error	Perc. Error (%)
S _{BET}	0.392	0.011	0.003	24	6.6	1.8	26
D _p	0.021	0.16	0.22	132	12	2	15
V _p	0.572	12	2	17	3.0	1.9	61
C	0.337	0.090	0.024	27	6.7	1.9	29
C·S _{BET}	0.780	1.7 E ⁻⁴	0.2 E ⁻⁴	10	5.4	0.9	17
C·V _p	0.578	0.089	0.015	17	7.6	1.1	15

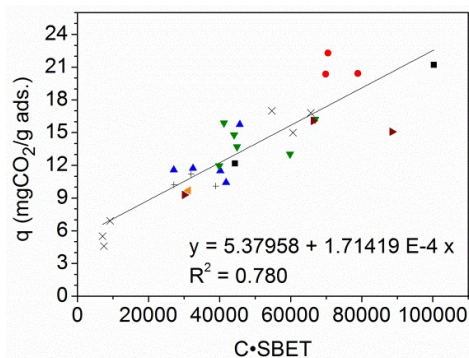


Fig 7. Linear regression of C·S_{BET} and CO₂ uptake values at 45 °C and 1 bar. Legend: conventional SBA-15 (■), Al-SBA-15 (●), pore-expanded SBA-15 (▲), HMS (▼), Silica Gel (◆), MCM-41 (▶), grafted SBA-15 (X) and co-condensed SBA-15 (+).

now much better fitted to a straight line, with no significant scattering. Also, the value of R² fitting parameter is much higher than those resulting from fitting the CO₂ uptake against individual textural parameters. A similar correlation was obtained considering the product of C and V_p, but the fitting was not so good (see Table 3).

The correlation between CO₂ uptake and the product of C and surface area in the present study is still valid at pressures higher than the atmospheric. When data at 4.5 bar were considered, the fitting showed an R² value of 0.818, much higher than any of the other correlations previously considered.

Finally, to investigate the possibility of mixed interactions between textural parameters, multivariable fittings ($y = \alpha \cdot x_1 + \beta \cdot x_2$) were studied, with y being the CO₂ uptake in all cases. In the first two experiments, C parameter was selected as the first independent variable (x₁), with S_{BET} and V_p being considered as the second variable (x₂). Two additional multivariable fitting were carried out, considering the product between surface area and C parameter as one independent variable and either V_p or S_{BET} as the second one. However, none of these correlations yielded substantial increases in the goodness of the fit compared to the previous one shown in Figure 7. Moreover, they entailed higher relative errors in the parameters obtained, so it can be inferred that adding the influence of these variables does not significantly improve the fitting.

All things considered, it can be concluded that in an extensive number of materials, physisorbed CO₂ can be directly related to the combined influence of the available surface area (S_{BET}) and the affinity of this surface towards physisorption (C parameter), measured in a simple way by means of the BET equation (C·S_{BET}).

When mesoporous silica adsorbents are used for CO₂ capture presenting just physisorption mechanism, with no chemical contribution, a linear relationship between CO₂ uptake and the product of C parameter and BET surface was established. As a uniform rule inferred from the fitting in Figure 7, it can be concluded that at 45°C and 1 bar the linear dependence was found to be:

$$q_{CO_2} = 1.714 \cdot 10^{-4} (S_{BET} \cdot C) + 5.38 \quad 5$$

It is noteworthy to remark that this finding is in agreement with the well-known surface-dependent nature of physical adsorption, which explains the dependence of the gas uptake on both the available surface and the adsorption potential.¹⁷ Moreover, this is an important outcome, since the CO₂ uptake of a mesostructured material can be predicted from its textural properties using Equation 5.

This correlation explains for example, that SBA-BT and HMS-10c exhibited almost the same CO₂ adsorption capacity (15.0 and 14.8 mg/g) but having significantly different values of BET surface and C parameter (612 m²/g and 99 for the former; and 918 m²/g and 48 for the latter). That means that the same CO₂ uptake can be obtained with materials having few physical sorption sites (accounted by the BET surface area)

with high affinity or else with adsorbents displaying many physisorption sites, although less active.

Conclusions

In this work, more than 30 physisorbents were subjected to N₂ adsorption at -193 °C and CO₂ adsorption at 45 °C. The CO₂ uptake of these samples was found to correlate with their textural parameters, namely the product of the available surface area (S_{BET}) and the affinity of the surface toward adsorptives (C parameter). Although R² values obtained for this linear fitting are not too high (0.78 and 0.82 at 1 bar and 4.5 bar respectively), the correlation found is significant taking into account that more than 30 materials prepared by a variety of procedures were considered. This is a novel finding that allows the estimation of CO₂ uptake values from physical adsorbents based on mesostructured silicas directly from their textural properties. The significance of this new correlation lies in the industrial importance of post-combustion CO₂ capture, an application for which all these materials have been extensively proposed.

Notes and references

- J. Wang, L. Huang, R. Yang, Z. Zhang, J. Wu, Y. Gao, Q. Wang, D. O'Hare, Z. Zhong, *Energy Environ. Science*, 2014, **7**, 3478.
- A. Samanta, A. Zhao, G.K.H. Shimizu, P. Sarkar, R. Gupta, *Ind. Eng. Chem. Res.*, 2012, **51**, 1438.
- S. Choi, J.H. Drese, C.W. Jones, *ChemSusChem*, 2009, **2**, 796.
- N. Chalal, H. Bouhali, H. Hamaizi, B. Lebeau, A. Bengueddach, *Microporous Mesoporous Mater.*, 2015, **210**, 32.
- A. Erto, A. Silvestre-Albero, J. Silvestre-Albero, F. Rodríguez-Reinoso, M. Balsamo, A. Lancia, F. Montagnaro, *J. Colloid Interface Sci.*, 2015, **448**, 41-50.
- R.V. Siriwardane, M.S. Shen, E.P. Fisher, J.A. Poston, *Energy Fuels*, 2001, **15**, 279.
- Y. Belmabkhout, G. De Weireld, A. Sayari, *Langmuir*, 2009, **25**, 13275.
- S. Yang, J. Sun, A.J. Ramírez-Cuesta, S.K. Cleave, W.I.F. David, D.P. Anderson, R. Newby, A.J. Blake, J.E. Parker, C.C. Tang, M. Schröder, *Nat. Chem.*, 2012, **4**, 887.
- E.S. Sanz-Pérez, M. Olivares-Marín, A. Arencibia, R. Sanz, G. Calleja, M.M. Maroto-Valer, *Int. J. Greenh. Gas Control*, 2013, **17**, 366.
- D.M. Ruthven, *Principles of Adsorption and Adsorption Processes*, Wiley Interscience, New York, 1984.
- S. Brunauer, P.H. Emmett, E. Teller, *J. Amer. Chem. Soc.*, 1938, **60**, 309.
- M. Thommes, K. Kaneko, A.V. Neimark, J.P. Olivier, F. Rodríguez-Reinoso, J. Rouquerol and K.S. W. Sing, *Pure Appl. Chem.*, 2015, **87**, 1051.
- F. Salvador, C. Sánchez-Jiménez, M.J. Sánchez-Montero, A.A. Salvador, *Stud. Surf. Sci. Catal.*, 2002, **144**, 379.
- M.J. Remy, G.A.A. Poncelet, *J. Phys. Chem.*, 1995, **99** (2), 773.
- S.J. Gregg, K.S.W. Sing, *Adsorption, Surface Area and Porosity*, second ed., Academic Press Inc., London, 1982.
- K.S.W. Sing, D.H. Everett, R.A.W. Haul, L. Moscou, R.A. Pierotti, J. Rouquerol, T. Siemieniowska, *Pure Appl. Chem.*, 1985, **57**, 603.
- A. Ansón, J. Jagiello, J.B. Parra, M.L. Sanjuán, A.M. Benito, W.K. Maser, M.T. Martínez, *J. Phys. Chem. B*, 2004, **108**, 15820.
- R. Ströbel, L. Jörissen, T. Schliermann, V. Trapp, W. Schütz, K. Bohmhammel, G. Wolf, J.J. Garche, *Power Sources*, 1999, **84**, 221.
- A. Züttel, P. Sudan, P. Mauron, P. Wenger, *Appl. Phys. A*, 2004, **78**, 941.
- M. Rzepka, P. Lamp, M.A. de la Casa-Lillo, *J. Phys. Chem. B*, 1998, **102** (52), 10894.
- T.C. Drage, A. Arenillas, K.M. Smith, C. Pevida, S. Piippo, C.E. Snape, *Fuel*, 2007, **86**, 22.
- M. Sereych, J. Lison, U. Jans, T.J. Bandoz, *Carbon*, 2009, **47**, 2491.
- J.B. Parra, C.O. Ania, A. Arenillas, F. Rubiera, J.M. Palacios, J.J. Pis, *J. Alloys Compd.*, 2004, **379**, 280.
- R. Gadiou, S.E. Saadallah, T. Piquero, P. David, J. Parmentier, C. Vix-Guterl, *Microporous Mesoporous Mater.*, 2005, **79**, 121.
- J. Kim, L.-C. Lin, J.A. Swisher, M. Haranczyk, B. Smit, *J. Am. Chem. Soc.*, 2012, **134** (46), 18940.
- C.C. Ahn, Y. Ye, B.V. Ratnakumar, C. Witham, R.C. Bowman Jr., B. Fultz, *Appl. Phys. Lett.*, 1998, **73** (23), 3378.
- M. Bastos-Neto, D.V. Canabrava, A.E.B. Torres, E. Rodríguez-Castello, A. Jiménez-López, D.C.S. Azevedo, C.L. Cavalcante Jr., *Appl. Surf. Sci.*, 2007, **253**, 5721.
- M. Jordá-Beneyto, F. Suárez-García, D. Lozano-Castelló, D. Cazorla-Amorós, A. Linares-Solano, *Carbon*, 2007, **45**, 293.
- C. Xu, N. Hedin, *J. Mater. Chem. A*, 2013, **1** (10), 3406.
- A.A. Alhwaige, T. Agag, H. Ishida, S. Qutubuddin, *RSC Adv.*, 2013, **3**, 16011.
- R. Gaikwad, W.L. Boward, W. DePriest, National Lime Association. Sargent & Lundy, Chicago, 2003.
- D. Zhao, J. Feng, Q. Huo, N. Melosh, G. Fredrickson, B. Chmelka and G. Stucky, *Science*, 1998, **279**, 548-52.
- Y. Yue, A. Gédéon, J.-L. Bonardet, J.-B. D'Espinose, J. Fraissard and N. Melosh, *Chem. Commun.*, 1999, 1967-8.
- L. Cao, T. Man and M. Kruk, *Chem. Mater.*, 2009, **21**, 1144-53.
- W. Lin, Q. Cai, W. Pang, Y. Yue and B. Zou, *Microporous Mesoporous Mater.*, 1999, **33**, 187-196.
- M. Kruk, M. Jaroniec and A. Sayari, *Microporous Mesoporous Mater.*, 2000, **35-36**, 545-553.
- P. T. Tanev and T. J. Pinnavaia, *Science* (80-), 1995, **267**, 865-7.
- V. Ya Davidov, A.V. Kiselev, L.T. Zhuravlev, *Trans. Faraday Soc.*, 1964, **60**, 2254.
- L.T. Zhuravlev, *Langmuir*, 1987, **3**, 316.
- J. Chaignon, Y. Bouizi, L. Davin, N. Calin, B. Albela, L. Bonneviot, *Green Chem.*, 2015, **17**, 3130.
- R. Sanz, G. Calleja, A. Arencibia, E.S. Sanz-Pérez, *Microporous Mesoporous Mater.*, 2012, **158**, 309.
- A.S. Maria Chong, X.S. Zhao, A.T. Kustedjo, S.Z. Qiao, *Microporous Mesoporous Mater.*, 2004, **72**, 33.
- S.A. Didas, A.R. Kulkarni, D.S. Sholl, C.W. Jones, *ChemSusChem*, 2012, **5**, 2058.
- M. Caplow, *J. Am. Chem. Soc.*, 1968, **24**, 6795.
- R. Serna-Guerrero, Y. Belmabkhout, A. Sayari, *Chem. Eng. J.*, 2010, **161**, 173.
- R. Sanz, G. Calleja, A. Arencibia, E.S. Sanz-Pérez, *Energy Fuels*, 2013, **27**, 7637.
- B. Aziz, N. Hedin, Z. Bacsik, *Microporous Mesoporous Mater.*, 2012, **150**, 42-49.
- R. Sips, *J. Chem. Phys.*, 1948, **16**, 490.

- 49 S. K. Papageorgiou, F. K. Katsaros, E. P. Kouvelos, J. W. Nolan, H. Le Deit and N. K. Kanellopoulos, *J. Hazard. Mater.*, 2006, **137**, 1765–72.
- 50 W. Rudzinski and D. H. Everett, *Adsorption of Gases on Heterogeneous Surfaces*, Elsevier, 1992.
- 51 G. P. Knowles, J. V. Graham, S. W. Delaney and A. L. Chaffee, *Fuel Process. Technol.*, 2005, **86**, 1435–48.
- 52 C. Knöfel, C. Martin, V. Hornebecq and P. L. Llewellyn, *J. Phys. Chem. C*, 2009, **113**, 21726–34.
- 53 G. P. Knowles, S. W. Delaney and A. L. Chaffee, *Ind. Eng. Chem. Res.*, 2006, 2626–33.
- 54 O. Leal, C. Bolívar, G. Sepúlveda, G. Molleja, G. Martínez, L. Esparragoza. EE.UU. Patent 2.087.597 (1992).
- 55 A.C.C. Chang, S.S.C. Chuang, M. Gray, Y. Soong. *Energy Fuels* (2003) **17**, 468-473.
- 56 W. Klinthong, C.-H. Huang, C.-S. Tan, *Microporous Mesoporous Mater.*, 2014, **197**, 278.
- 57 J. Fujiki, H. Yamada, K. Yogo, *Microporous Mesoporous Mater.*, 2015, **215**, 76.
- 58 N. Minju, P. Abhilash, B.N. Nair, A.P. Mohamed, S. Ananthakumar, *Chem. Eng. J.*, 2015, **269**, 335.
- 59 E. Vilarrasa-García, E.M.O. Moya, J.A. Cecilia, C.L., Jr. Cavalcante, J. Jiménez-Jiménez, D.C.S. Azevedo, E. Rodríguez-Castellón, *Microporous Mesoporous Mater.*, 2015, **209**, 172.
- 60 J.A.A. Gibson, A.V. Gromov, S. Brandani, E.E.B. Campbell, *Microporous Mesoporous Mater.*, 2015, **208**, 129.
- 61 E.G. Moschetta, M.A. Sakwa-Novak, J.L. Greenfield, C.W. Jones, *Langmuir*, 2015, **31**, 2218.
- 62 A.L. Chaffee, *Fuel Process. Technol.*, 2005, **86**, 1473.
- 63 G.P. Knowles, S.W. Delaney, A.L. Chaffee, *Ind. Eng. Chem. Res.*, 2006, **45**, 2626.
- 64 P.J.E. Harlick, A. Sayari, *Ind. Eng. Chem. Res.*, 2007, **46**, 446.
- 65 W. Lu, J.P. Sculley, D. Yuan, R. Krishna, Z. Wei, H.-C. Zhou, *Angewandte Chemie (Int. Ed.)*, 2012, **51(30)**, 7480.
- 66 M. Sevilla, J. B. Parra, A. B. Fuertes, *ACS Appl. Mater. Interfaces*, 2013, **5**, 6360.
- 67 V. Presser, J. McDonough, S.-H. Yeon, Y. Gogotsi, *Energy Environ. Sci.*, 2011, **4**, 3059.
- 68 A. Silvestre-Albero, S. Rico-Francés, F. Rodríguez-Reinoso, A. M. Kern, M. Klumpp, B. J. M. Etzold, J. Silvestre-Albero, *Carbon*, 2013, **59**, 221.

